Spin-coherence time measurements of NV^- centers in $_{15}N^+$, $_{15}N_2^+$ and O^+ implanted diamond

S. B. Lisesivdin [a,b,*], J. Lang [b,c], F. Jelezko [b,c]

[a] *Gazi University, Faculty of Science, Department of Physics, 06500, Teknikokullar, Ankara, Turkey.*
[b] *Institute for Quantum Optics, Ulm University, D-89081 Germany*
[c] *Center for Integrated Quantum Science and Technology (IQst), Ulm University, D-89081 Germany*

*: Corresponding Author: Sefer Bora Lisesivdin; Tel: +903122021391; Email: sblisesivdin@gmail.com

Abstract

For the solid-state qubit studies, NV- defects in the diamond are one of the most promising and most studied candidates. With its stable negative charge state, long coherence time at room temperature and spectral stability properties, the fabrication of NV- defects with improving these properties are getting more importance. In this study, NV- centers with introducing Oxygen impurity nearby an NV- center. Required Nitrogen and Oxygen impurities are implanted into diamond samples as $_{15}N^+$, $_{15}N_2^+$ and O^+ ions with different ion flux values. Nitrogen impurities and oxygen impurities are merged into a lattice with the separate annealing processes. Optically detected magnetic resonance (ODMR), Rabi oscillation and Hahn echo measurements are performed. The coherence times up to 78 μs are reported.

Introduction

The nitrogen-vacancy (NV) center is an separately addressable electronic spin in bulk and nanocrystalline diamond that can be initialized and read out with optical excitation [1] and coherently controlled with microwave RF signal [2] at even room temperature. With its exceptionally long spin coherence times (T_2) of NV centers in isotopically engineered materials [3]. These features enable the detection of weak coupling between single NV centers and other quantum degrees of freedom, resulting a possibility of wide variety of different applications. These applications of NV center spins can be listed as nanoscale magnetoprobes include electric-field sensing [4], magnetic imaging [5], magnetometry, [6] and thermometry [7].

Instead of being limited to NV centers formed during diamond growth (mostly with microwave-plasma-assisted chemical vapor deposition (MW-PECVD)) , they can be created, for example by separate nitrogen ion implantation. Nitrogen ion implantation results an NV positioning accuracy that motivates integration with on-chip photonics and coupling between other nearby NV centers. Precise locating of these NV centers or accurately locating their position is also a prerequisite for optimal overlap of the dipole with the electric field mode of diamond optical cavities, for enhancing light-matter interaction better. Also, ion implantation allows for the creation of single NV centers in high purity diamond, providing a potentially low-defect system.

Spin coherence at shallow depths (<10 nm) is affected by the surface characteristics of the crystal. Some essential methodologies for etching, passivating, and cleaning surfaces of NV-doped diamond are used for nanoscale magnetoprobes applications listed above. Previously, efforts of surface treatment by plasma or thermal oxidation have been made to stabilize the NV charge state [8-9].

In this study, we used oxygen implantation in addition to nitrogen implantation to make the oxygen more localized with nitrogen and therefore may help to stabilize the NV charge state.

Methods

The sample used in this study was a high-purity (Nitrogen concentration <1 ppb) and isotopically purified (^{12}C 99.998%) homoepitaxial (100) diamond film grown by MW-PECVD at University of Ulm. Ionized nitrogen and oxygen molecules, $^{15}N^+$, $^{15}N^{2+}$, and O^+ were implanted into the diamond with an acceleration voltage of 5 keV. The spot is kept nearly 70 μm. The ion fluences were 0.0, 5.0×10^8, 5.0×10^9, and 5.0×10^{10} for Oxygen, 5.0×10^8, 5.0×10^9, and 5.0×10^{10} for $^{15}N^+$, and 5.0×10^8, and 5.0×10^{10} for $^{15}N^{2+}$.

Nitrogen implantations were done after Oxygen implantation and the sample was annealed after Oxygen implantation and Nitrogen implantation at 1000 °C for 3h and 1200 °C for 1h, respectively. Before further measurements, sample is cleaned with Piranha solution for 1h.

The details of the sample is shown in Figure 1.

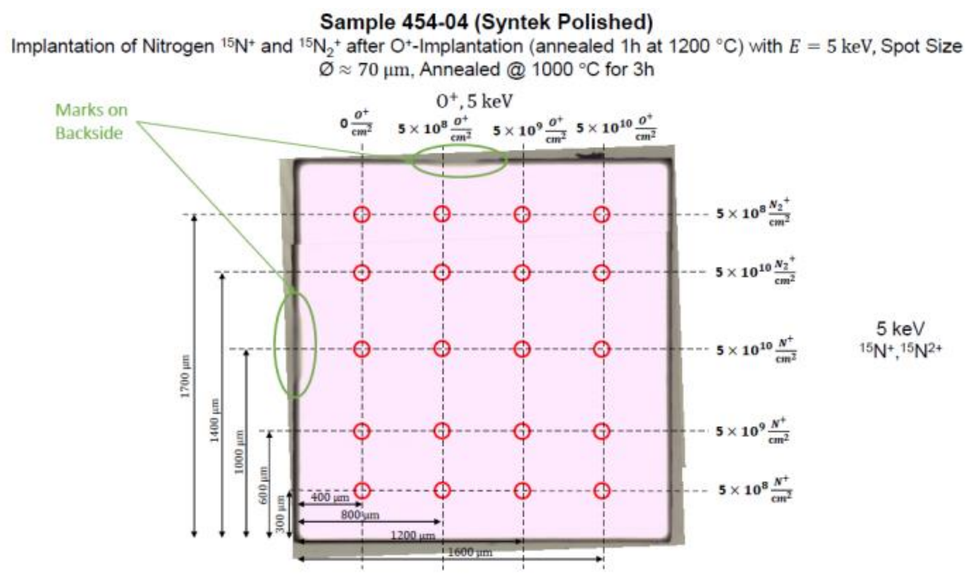

Figure 1 Studied sample with 20 different oxygen and nitrogen implantation ion fluxes. Coordinates of the implanted areas are also shown.

Results

Due to the simulated distribution of implanted ions and vacancies as computed by the SRIM code (Stopping and Range of Ions in Matter, version 2008), the average depth of individual ions with 5 keV acceleration voltage is calculated as 5-10 nm.

After annealing and etch cleaning, the resultant NV centers were measured using a home-built confocal microscope located at University of Ulm and the spin properties were observed through optically detected magnetic resonance (ODMR) spectroscopy. Observation of either the implanted ^{15}N hyperfine structure (with nuclear spin, I = 1/2) or native ^{14}N (I = 1, natural abundance 99.63%) by ODMR spectroscopy allowed determination of whether the investigated NV centers were due to implantation or pre-existing impurities in the substrate.

A confocal image of the co-implanted region is shown in Fig. 2. For every point show in figure 1, tens of confocal measurements including ODMR, Rabi pulse measurements and Hahn echo measurements were taken. From Hahn echo measurements, lifetimes show a disperse between 23-48 μs for areas without Oxygen implantation. With Oxygen implantation, this value increases up to 78 μs. In figure 2, the confocal measurements of 5.0×10^{10} flux Oxygen and 5.0×10^{10} flux $^{15}N^+$ point is shown as an example.

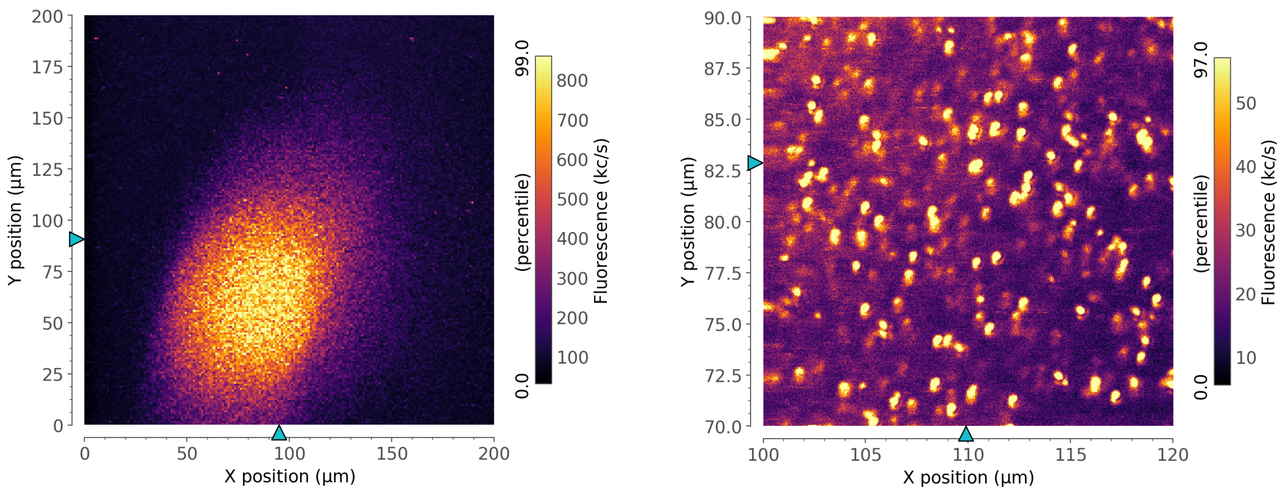

Figure 2 Sample confocals of the studied sample. (Left) Spot size of 70 μm can be observed. (Right) Individual NV centers.

For the ODMR, Rabi pulse and Hahn echo results, we report here the area with the maximum lifetime observed, which is with 5.0×10^{10} flux Oxygen and 5.0×10^8 flux $^{15}N^+$ fluxes in Figure 3 and Figure 4.

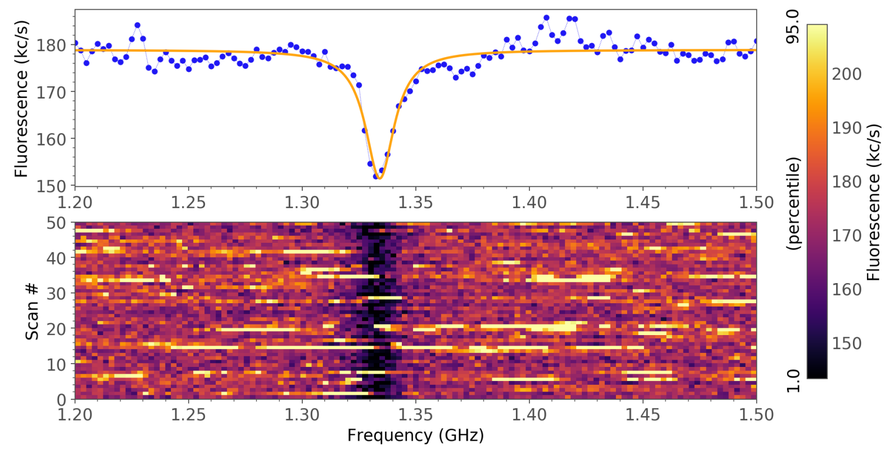

Figure 3 ODMR measurement for the area with 5.0×10^{10} flux Oxygen and 5.0×10^8 flux $^{15}N^+$ fluxes.

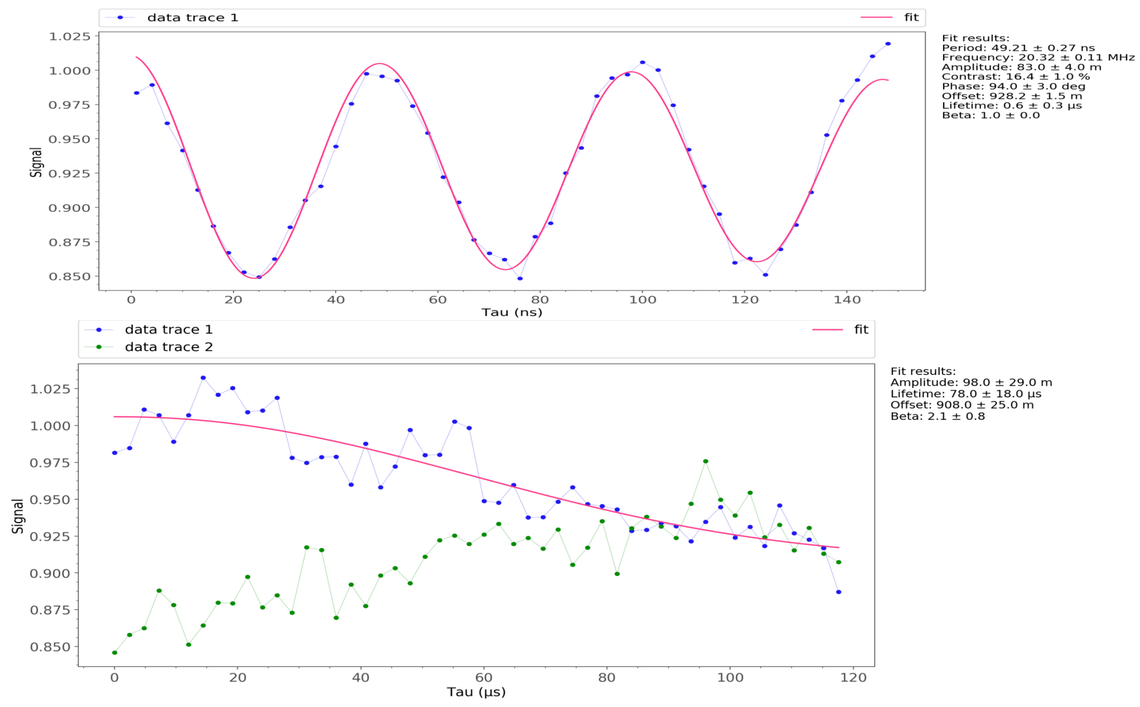

Figure 4 (Up) Rabi pulse and (Down) Hahn echo measurements for the area with 5.0×10^{10} flux Oxygen and 5.0×10^8 flux $^{15}N^+$ fluxes.

Conclusion

Hahn echo was performed on each NV and the decay curves were fitted by $E(2\tau) \propto exp[-(2\tau/T_2)^{\alpha}]$ where α is a free parameter. The long coherence times of Oxygen implanted samples of 78 ± 18 μs, to the best of our knowledge, increased coherence times, with respect to shallow implanted NV centers without Oxygen implantation.

Acknowledgments

S.B.L was supported in part by the Distinguished Young Scientist Award of the Turkish Academy of Sciences (TUBA-GEBIP 2016).

References

[1] A. Gruber, A. Drabenstedt, C. Tietz, L. Fleury, J. Wrachtrup, and C. von Borczyskowski, Science 276, 2012 (1997).
[2] F. Jelezko, T. Gaebel, I. Popa, A. Gruber, and J. Wrachtrup, Phys. Rev. Lett. 92, 076401 (2004).
[3] G. Balasubramanian, P. Neumann, D. Twitchen, M. Markham, R. Kolesov, N. Mizuochi, J. Isoya, J. Achard, J. Beck, J. Tissler, V. Jacques, P. R. Hemmer, F. Jelezko, and J. Wrachtrup, Nat. Mater. 8, 383 (2009).
[4] F. Dolde, H. Fedder, M. W. Doherty, T. Nobauer, F. Rempp, G. Balasubramanian, T. Wolf, F. Reinhard, L. C. L. Hollenberg, F. Jelezko, and J. Wrachtrup, Nat. Phys. 7, 459 (2011).
[5] P. Maletinsky, S. Hong, M. S. Grinolds, B. Hausmann, M. D. Lukin, R. L. Walsworth, M. Loncar, and A. Yacoby, Nat. Nanotechnol. 7, 320 (2012).
[6] J. M. Taylor, P. Cappellaro, L. Childress, L. Jiang, D. Budker, P. R. Hemmer, A. Yacoby, R. Walsworth, and M. D. Lukin, Nat. Phys. 4, 810 (2008).
[7] D. M. Toyli, D. J. Christle, A. Alkauskas, B. B. Buckley, C. G. Van de Walle, and D. D. Awschalom, Phys. Rev. X 2, 031001 (2012).
[8] S. Cui and E. L. Hu, Appl. Phys. Lett. 103, 051603 (2013).
[9] K. M. C. Fu, C. Santori, P. E. Barclay, and R. G. Beausoleil, Appl. Phys. Lett. 96, 121907 (2010).